Taylor & Francis
Taylor & Francis Group

Automatika

Journal for Control, Measurement, Electronics, Computing and Communications

ISSN: (Print) (Online) Journal homepage: https://www.tandfonline.com/loi/taut20

Efficiency improvement of a three-coil WPT system with rectified load based on a selected compensation capacitor

Han Liu & Jing Lu

To cite this article: Han Liu & Jing Lu (2023) Efficiency improvement of a three-coil WPT system with rectified load based on a selected compensation capacitor, Automatika, 64:1, 73-78, DOI: 10.1080/00051144.2022.2102513

To link to this article: https://doi.org/10.1080/00051144.2022.2102513

Published online: 20 Jul 2022.

AUTOMATIKA
2023, VOL. 64, NO. 1, 73–78
https://doi.org/10.1080/00051144.2022.2102513

REGULAR PAPER

OPEN ACCESS Check for updates

Efficiency improvement of a three-coil WPT system with rectified load based on a selected compensation capacitor

Han Liu[a,b] and Jing Lu[c]

[a]College of Energy and Electrical Engineering, Hohai University, Nanjing, People's Republic of China; [b]Jiangsu Provincial Key Laboratory of Smart Grid Technology and Equipment, Southeast University, Nanjing, People's Republic of China; [c]Changzhou Power Supply Branch, State Grid Jiangsu Electric Power Co., Ltd., Changzhou, People's Republic of China

ABSTRACT

In the existing pieces of literature about the three-coil wireless power transfer (WPT) system, a three-coil structure is proposed to increase the efficiency compared to the two-coil WPT system. The cross-coupling among three coils, compensation capacitor of the repeating coil (RPC) and the rectified load are considered incompletely. The circuit model of a three-coil WPT system with rectified load is developed by taking the cross-coupling of all coils and the compensation capacitor of RPC into consideration in this paper. The relationship among system efficiency, compensation level, and rectifier load is deduced. The detailed mathematical analysis and compensation capacitor selection of RPC are investigated to improve the system efficiency. An experimental study demonstrates that the selected compensation capacitor of RPC achieves a higher efficiency than resonant compensation in a three-coil WPT system with different cross-coupling conditions and rectifier load conditions. System efficiency is promoted from 73.9% (resonant compensation capacitor for RPC) to 84.2% (selected compensation capacitor for RPC).

ARTICLE HISTORY
Received 18 January 2022
Accepted 12 July 2022

KEYWORDS
Wireless power transfer; compensation capacitor selection; rectified load; cross-coupling

1. Introduction

The wireless power transfer (WPT) technology has been developed rapidly these years [1–4]. It can realize the transmission of electric energy across the air compared with the traditional contact mode. Especially the inductive power transfer based on the magnetic-field coupling is the most popular WPT technology [5–8]. The WPT technology has been applied in many areas, such as industrial robots [9,10], electric vehicles [11–13], consumer electronics, implantable equipment, unmanned underwater devices, etc.

Based on the two-coil WPT system, the three-coil [14] or multi-coil [15] structures are proposed to promote the system efficiency when the distance between the transmitting coil and receiving coil increases. In the three-coil structure WPT, the application of a repeating coil (RPC) can reduce the current in the drive circuit [14,16,17]. For the three-coil WPT system with RPC composed of double coils in [18], the constant current and constant voltage modes are realized based on the reconfigurable middle coil. In [19], a switch device is used in the receiving end to select the constant current mode or the constant voltage mode in the WPT system with RPC.

In the existing pieces of literatures about the three-coil WPT system, the cross-coupling between the transmitting coil (TC) and receiving coil (RC) is usually ignored to simplify the analysis of the modelling [14]. In [20] where the cross-coupling and rectifier of load are ignored, the efficiency optimization and power stability of a WPT system charging multiple loads with a relay coil structure are studied, and the frequency configuration and distribution design are proposed. To investigate the comprehensive characteristics of a three-coil WPT system, the cross-coupling among all three coils and rectifier loads should be considered in the modelling and analysis process. On the other hand, RPC is commonly compensated resonantly with a series capacitor [14,20]. The analysis and selection for compensation capacitors of RPC are also rarely discussed to promote system efficiency.

To fill this gap, the efficiency improvement of a three-coil WPT system with rectified load based on a selected compensation capacitor is investigated in this paper. This paper is organized as follows. In Section II, the circuit model of a three-coil WPT system with a rectifier load, considering the cross-coupling of three coils and a compensation capacitor of RPC, is developed. In Section III, the relationship among system efficiency, compensation capacitor of RPC and rectifier load is deduced. The detailed mathematical analysis and compensation capacitor selection of RPC is investigated to improve the system efficiency. In Section IV, the theoretical research is verified by experiments with different cross-coupling and rectifier load conditions. Finally, conclusions are summarized in Section V.

CONTACT Han Liu liuhanhh@hhu.edu.cn

2. Modelling of a three-coil WPT system with a non-resonant repeating coil

The typical circuit diagram of a three-coil WPT system is introduced in Figure 1. The equivalent circuit of the three-coil WPT system with non-resonant compensated RPC considering all cross-couplings is shown in Figure 1. U_s represents the output voltage of a high-frequency inverter. L_t and R_t represent the inductance and internal resistance of TC, respectively. The *LCC* (inductor-capacitor-capacitor) compensation circuit at the transmission side is composed of L_f, C_f, and C_t. L_r and R_r are the inductance and internal resistance of RC, respectively. C_r represents the compensation capacitance at the receiving side. R_{L} (the equivalent AC load in Figure 2) can be converted by R_{DC} (DC load after rectifier in Figure 1) according to $R_L = (8R_{\mathrm{DC}})/(\pi^2)$ [21]. The inductance and the resistance of RPC are L_2 and R_2, respectively.

The compensation capacitor C_2 is connected in series. k_1 and k_2 represent the coupling coefficient between TC and RPC and that between RC and RPC, respectively. k_3 is the coupling coefficient between TC and RC. The system works at the frequency of f. The corresponding angular frequency is $\omega = 2\pi f$.

In Figure 2, $\mathbf{I}_f$ is the output current of the inverter. $\mathbf{I}_t$, $\mathbf{I}_2$ and $\mathbf{I}_r$ are the currents of TC, RPC, and RC, respectively. The following circuit equation can be derived based on the mesh current analysis

$$\begin{aligned}&(Z_{Lf}+Z_{Cf})\mathbf{I}_f - Z_{Cf}\mathbf{I}_t\\ &\quad = U_s - Z_{Cf}\mathbf{I}_f + (Z_{Lt}+Z_{Ct}+Z_{Cf}+R_t)\mathbf{I}_t\\ &\qquad - Z_{k1}\mathbf{I}_2 - Z_{k3}\mathbf{I}_r = 0\end{aligned}$$

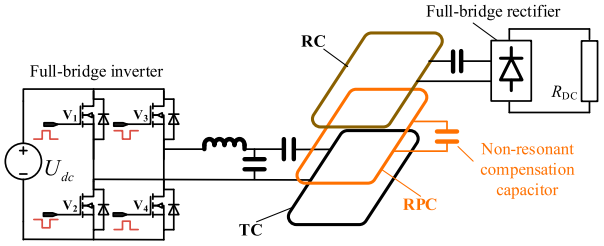

Figure 1. The typical circuit diagram of a three-coil WPT system.

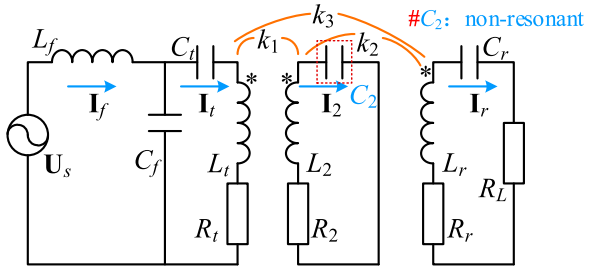

Figure 2. Equivalent circuit of a three-coil WPT system with non-resonant compensated RPC considering all cross-couplings.

$$\begin{aligned}&- Z_{k1}\mathbf{I}_t + (Z_{L2}+Z_{C2}+R_2)\mathbf{I}_2 - Z_{k2}\mathbf{I}_r = 0\\ &- Z_{k3}\mathbf{I}_t - Z_{k2}\mathbf{I}_2\\ &+ \left(Z_{Lr}+Z_{Cr}+R_r+\frac{8R_{\mathrm{DC}}}{\pi^2}\right)\mathbf{I}_r = 0\end{aligned} \tag{1}$$

where $Z_{Lt} = j\omega L_t$, $Z_{Ct} = 1/(j\omega C_t)$, $Z_{Lf} = j\omega L_f$, $Z_{Cf} = 1/(j\omega C_f)$, $Z_{L2} = j\omega L_2$, $Z_{C2} = 1/(j\omega C_2)$, $Z_{Lr} = j\omega L_r$, $Z_{Cr} = 1/(j\omega C_r)$, $Z_{k1} = jX_{k1} = j\omega k_1\sqrt{L_tL_2}$, $Z_{k2} = jX_{k2} = j\omega k_2\sqrt{L_2L_r}$, $Z_{k3} = jX_{k3} = j\omega k_3\sqrt{L_tL_r}$.

The compensation topology on the transmitting side is *LCC* type and the parameter [22] satisfies

$$\omega = \frac{1}{\sqrt{L_fC_f}} = \frac{1}{\sqrt{(L_t-L_f)C_t}}. \tag{2}$$

According to (1) and (2), the current of TC can be calculated by

$$I_t = \frac{U_s}{\omega L_f}. \tag{3}$$

The series resonant compensation circuit is applied on the receiving side, which satisfies

$$\omega = \frac{1}{\sqrt{L_rC_r}}. \tag{4}$$

U' and U'' represent the induced voltages produced in the RPC circuit and RC circuit by the TC circuit, respectively.

$$\begin{aligned}U' &= Z_{k1}\cdot\mathbf{I}_t = U_sk_1\sqrt{L_tL_2}/L_f\\ U'' &= Z_{k3}\cdot\mathbf{I}_t = U_sk_3\sqrt{L_tL_r}/L_f\end{aligned} \tag{5}$$

In general, the compensation circuit is designed resonantly according to the operating frequency of the system. The compensation capacitor of RPC is rarely investigated in a three-coil WPT system with a rectifier load. In this paper, the selection of compensation capacitor is discussed in detail considering all cross-couplings among three coils and a rectifier load.

Parts of (1) can be rewritten as

$$\begin{cases}(R_2+j(\omega L_2-1/(\omega C_2)))\cdot\mathbf{I}_2 - Z_{k2}\cdot\mathbf{I}_r = U'\\ -Z_{k2}\cdot\mathbf{I}_2 + \left(R_r+\dfrac{8R_{\mathrm{DC}}}{\pi^2}\right)\cdot\mathbf{I}_r = U''\end{cases}. \tag{6}$$

The current at the receiving side can be deduced by

$$\begin{aligned}\mathbf{I}_r &= \frac{U''(R_2+j(\omega L_2-1/(\omega C_2)))+U'Z_{k2}}{\left(R_r+\frac{8R_{\mathrm{DC}}}{\pi^2}\right)(R_2+j(\omega L_2-1/(\omega C_2)))-{Z_{k2}}^2}\\ &= \frac{U_s}{L_f}\cdot\frac{\begin{array}{c}R_2k_3\sqrt{L_tL_r}+j\left((\omega L_2-1/(\omega C_2))\right.\\ \left.k_3\sqrt{L_tL_r}+\omega k_1k_2L_2\sqrt{L_tL_r}\right)\end{array}}{\begin{array}{c}\left(R_r+\frac{8R_{\mathrm{DC}}}{\pi^2}\right)R_2+\omega^2{k_2}^2L_2L_r\\ +j(\omega L_2-1/(\omega C_2))\left(R_r+\frac{8R_{\mathrm{DC}}}{\pi^2}\right)\end{array}}.\end{aligned} \tag{7}$$

The current of RPC can be represented by

$$\mathbf{I}_2 = \frac{U'(R_r + R_L) + U''Z_{k2}}{\left(R_r + \frac{8R_{\mathrm{DC}}}{\pi^2}\right)(R_2 + j(\omega L_2 - 1/(\omega C_2))) - {Z_{k2}}^2} = \frac{U_s}{L_f} \cdot \frac{\begin{array}{c}(R_r + R_L)k_1\sqrt{L_tL_2} \\ +j\omega k_2k_3L_r\sqrt{L_tL_2}\end{array}}{\begin{array}{c}\left(R_r + \frac{8R_{\mathrm{DC}}}{\pi^2}\right)R_2 + \omega^2{k_2}^2L_2L_r \\ +j(\omega L_2 - 1/(\omega C_2))\left(R_r + \frac{8R_{\mathrm{DC}}}{\pi^2}\right)\end{array}}. \quad (8)$$

The output power of the three-coil WPT system with a rectifier load is computed by

$$P = \frac{8R_{\mathrm{DC}}\mathbf{I}_r\mathbf{I}_r^*}{\pi^2}. \quad (9)$$

The system efficiency can be calculated by

$$\eta = \frac{\mathbf{I}_r\mathbf{I}_r^* 8R_{\mathrm{DC}}}{\pi^2R_t\mathbf{I}_t\mathbf{I}_t^* + \pi^2R_2\mathbf{I}_2\mathbf{I}_2^* + \mathbf{I}_r\mathbf{I}_r^*(\pi^2R_r + 8R_{\mathrm{DC}})}. \quad (10)$$

According to (7)–(10), the compensation capacitor C_2 of the RPC circuit, together with cross-coupling (k_1, k_2 and k_3), will affect the output power and system efficiency. The algebraic analysis and optimization will be proposed to analyse the influence of non-resonant compensation degree on system efficiency in the next part.

3. Analysis and selection of a compensation capacitor

The system efficiency can be calculated by

$$\eta = \frac{8R_{\mathrm{DC}}}{\pi^2R_t\chi_{\mathbf{I}} + (\pi^2R_r + 8R_{\mathrm{DC}})} \quad (11)$$

where the efficiency analysis factor $\chi_{\mathbf{I}} = \frac{|\mathbf{I}_t|^2 + \sigma|\mathbf{I}_2|^2}{|\mathbf{I}_r|^2}$, $\sigma = \frac{R_2}{R_t}$.

Based on (3), (7) and (8), we have

$$\frac{|\mathbf{I}_t|^2}{|\mathbf{I}_r|^2} = \frac{\begin{array}{c}((\pi^2R_r + 8R_{\mathrm{DC}})R_2 + \pi^2\omega^2{k_2}^2L_2L_r)^2 \\ +(\omega L_2 - 1/(\omega C_2))^2(\pi^2R_r + 8R_{\mathrm{DC}})^2\end{array}}{\begin{array}{c}\pi^4{R_2}^2\omega^2{k_3}^2L_tL_r + ((\omega L_2 - 1/(\omega C_2)) \\ \pi^2\omega k_3\sqrt{L_tL_r} + \pi^2\omega^2k_1k_2L_2\sqrt{L_tL_r}\big)^2\end{array}} \quad (12)$$

$$\frac{|\mathbf{I}_2|^2}{|\mathbf{I}_r|^2} = \frac{\begin{array}{c}(\pi^2R_r + 8R_{\mathrm{DC}})^2{k_1}^2L_tL_2 \\ +\pi^4\omega^2{k_2}^2{k_3}^2{L_r}^2L_tL_2\end{array}}{\begin{array}{c}\pi^4{R_2}^2{k_3}^2L_tL_r \\ +\big((\omega L_2 - 1/(\omega C_2))\pi^2k_3\sqrt{L_tL_r} \\ +\pi^2\omega k_1k_2L_2\sqrt{L_tL_r}\big)^2\end{array}} \quad (13)$$

The efficiency analysis factor can be expressed as

$$\chi_{\mathbf{I}} = \frac{\begin{array}{c}\omega^2{L_0}^2{R_a}^2\delta^2 + (R_aR_2 + \pi^2\omega^2{k_2}^2L_2L_r)^2 \\ +(\sigma\omega^2{k_1}^2L_tL_2{R_a}^2 + \sigma\pi^4\omega^4{k_2}^2{k_3}^2{L_r}^2L_tL_2)\end{array}}{\begin{array}{c}\pi^4{R_2}^2\omega^2{k_3}^2L_tL_r \\ +\big(\pi^2\omega^2\delta L_0k_3\sqrt{L_tL_r} \\ +\pi^2\omega^2k_1k_2L_2\sqrt{L_tL_r}\big)^2\end{array}} \quad (14)$$

where $R_a = \pi^2R_r + 8R_{\mathrm{DC}}$ and $\delta = (L_2 - 1/(\omega^2C_2))/L_0$. L_0 is the reference value.

It can be concluded from (11) that efficiency will decrease with the increase of $\chi_{\mathbf{I}}$. Therefore, a maximum value can be achieved for η when $\chi_{\mathbf{I}}$ is minimized. (14) can be rewritten as

$$\chi_{\mathbf{I}} = \frac{\mathrm{A}_1\delta^2 + \mathrm{A}_2}{\mathrm{B}_1\delta^2 + \mathrm{B}_2\delta + \mathrm{B}_3} \quad (15)$$

where $\mathrm{A}_1 = \omega^2{L_0}^2{R_a}^2$, $\mathrm{A}_2 = (R_aR_2 + \pi^2\omega^2{k_2}^2L_2L_r)^2 + \sigma\omega^2{k_1}^2L_tL_2R_a^2 + \sigma\pi^4\omega^4{k_2}^2{k_3}^2{L_r}^2L_tL_2$, $\mathrm{B}_1 = \pi^4\omega^4{L_0}^2{k_3}^2L_tL_r$, $\mathrm{B}_2 = 2\pi^4\omega^4L_0k_1k_2k_3L_rL_2L_t$, $\mathrm{B}_3 = \pi^4\omega^4{k_1}^2{k_2}^2{L_2}^2L_tL_r + \pi^4\omega^2{R_2}^2{k_3}^2L_tL_r$.

If the coupling between TC and RC is ignored (k_3 is 0), B_1 and B_2 in (15) are 0. (15) is written as $\chi_{\mathbf{I}} = \frac{\mathrm{A}_1\delta^2 + \mathrm{A}_2}{\mathrm{B}_3}$. $\chi_{\mathbf{I}}$ reaches a minimum value and efficiency is maximum when $\delta = 0$. Hence, when the coupling coefficient $k_3 = 0$, the system efficiency is maximum when RPC is resonant compensated ($\delta = 0$) theoretically.

In this paper, all cross-couplings are considered. A_1, A_2, B_1, B_2 and B_3 are all positive. The efficiency factor $\chi_{\mathbf{I}}$ in (15) is the function of δ (related to compensation capacitance of RPC loop). Taking the derivative of $\chi_{\mathbf{I}}$ with respect to δ gives

$$\chi_{\mathbf{I}}(\delta)' = \frac{\mathrm{A}_1\mathrm{B}_2\delta^2 + (2\mathrm{A}_1\mathrm{B}_3 - 2\mathrm{A}_2\mathrm{B}_1)\delta - \mathrm{A}_2\mathrm{B}_2}{(\mathrm{B}_1\delta^2 + \mathrm{B}_2\delta + \mathrm{B}_3)^2} \quad (16)$$

According to $\chi_{\mathbf{I}}(\delta)' = 0$ two extreme points can be obtained

$$\delta_1 = \frac{\mathrm{A}_2\mathrm{B}_1 - \mathrm{A}_1\mathrm{B}_3}{\mathrm{A}_1\mathrm{B}_2} - \sqrt{\left(\frac{\mathrm{A}_2\mathrm{B}_1 - \mathrm{A}_1\mathrm{B}_3}{\mathrm{A}_1\mathrm{B}_2}\right)^2 + \frac{\mathrm{A}_2}{\mathrm{A}_1}}$$

$$\delta_2 = \frac{\mathrm{A}_2\mathrm{B}_1 - \mathrm{A}_1\mathrm{B}_3}{\mathrm{A}_1\mathrm{B}_2} + \sqrt{\left(\frac{\mathrm{A}_2\mathrm{B}_1 - \mathrm{A}_1\mathrm{B}_3}{\mathrm{A}_1\mathrm{B}_2}\right)^2 + \frac{\mathrm{A}_2}{\mathrm{A}_1}} \quad (17)$$

The maximum value of $\chi_{\mathbf{I}}$ can be achieved at the point $\delta = \delta_1$ and the minimum value is achieved at the point $\delta = \delta_2$. The Vieta theorem tells us that when $\delta_1\delta_2 = -\frac{\mathrm{A}_2}{\mathrm{A}_1}$ and $\delta_1 < 0 < \delta_2$, δ_1 will lie in the over-compensation region and δ_2 will lie in the under-compensation region.

Based on L'Hopital's rule in mathematics, we have $\lim_{\delta \to -\infty} \chi_{\mathbf{I}}(\delta) = \lim_{\delta \to +\infty} \chi_{\mathbf{I}}(\delta) = \frac{\mathrm{A}_1}{\mathrm{B}_1}$, the minimum extreme point $\delta = \delta_2$ achieved by $\chi_{\mathbf{I}}$ is exactly the minimum value.

Therefore, the system efficiency will monotonically decrease for $\delta \in (-\infty, \delta_1)$, increase for $\delta \in (\delta_1, \delta_2)$, and decrease for $\delta \in (\delta_2, +\infty)$. The maximum value of efficiency is achieved at $\delta = \delta_2$ and the corresponding variation trend is presented in Table 1.

The theoretical optimal compensation degree δ_2 can be obtained by substituting the parameters in (15) and (17). In the RPC circuit, the compensation capacitor

Table 1. Change trend of the efficiency factor and system efficiency.

δ	$(-\infty, \delta_1)$	δ_1	(δ_1, δ_2)	δ_2	$(\delta_2, +\infty)$
χ_I	↗	MAX	↘	MIN	↗
η	↘	MIN	↗	MAX	↘

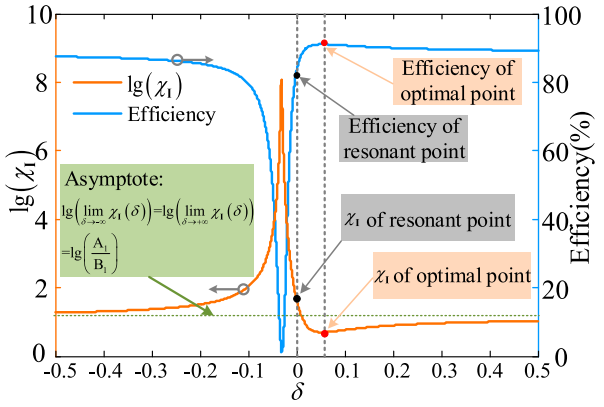

Figure 3. The characteristic curve of the efficiency factor (logarithmic form) and system efficiency as a function of the compensation degree factor δ.

corresponding to the optimal compensation degree factor can be calculated as $C_2 = \frac{1}{\omega^2(L_2 - \delta_2 L_0)}$.

According to (15) and (11), the efficiency factor χ_I (logarithmic form) and the system efficiency changing with the compensation degree of RPC are shown in Figure 3 (k_3 is not ignored). In Figure 3, the efficiency factor χ_I is at the minimum value when $\delta = \delta_2$ and the system efficiency is at the maximum value, demonstrating the correctness of the algebraic derivation analysis and optimization of the compensation degree.

4. Experimental verifications

The experimental prototype is built, as shown in Figure 4. The high-frequency full-bridge inverter is set up using DSP (TMS320F28335) as the controller and four MOSFETs (IRFP4227PBF). The full-bridge rectifier consists of four diodes (DSEP15-06A) on the receiving side. The system parameters are listed in Table 2. The external length of a side of three square coils is

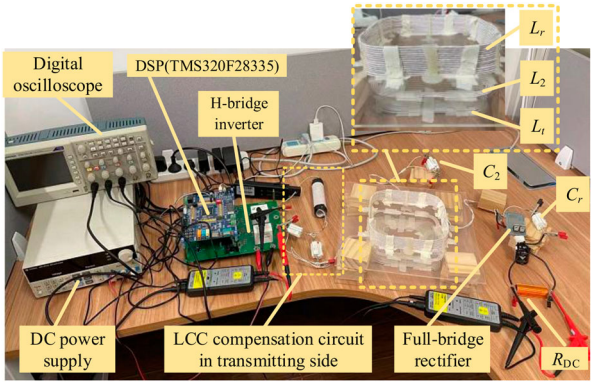

Figure 4. Experimental prototype.

Table 2. System parameters.

Symbol	L_t (μH)	L_r (μH)	L_2 (μH)	L_f (μH)	C_f (nF)
Value	43.6	64.4	6.8	17	149
C_t (nF)	C_r (nF)	U_s (V)	f (kHz)	L_0 (μH)	
95.3	39.4	20	100	10	

16 cm. The turns of the transmitting coil are 15. The turns of the repeating coil are 4. The turns of the receiving coil are 15.

After fixing the positions of three coils, mutual inductances are measured using an LCR meter (TH2817C). According to coil inductances, the cross-coupling can be obtained as $k_1 = 0.181$, $k_2 = 0.152$, $k_3 = 0.0672$. According to (15) and (17), the optimal compensation factor δ can be calculated as 0.1963 ($@R_{DC} = 5\Omega$) and 0.1188 ($@R_{DC} = 10\Omega$). The optimal compensation capacitors are 523.6 and 451.3 nF respectively, while the resonant compensation capacitor is 372.5 nF. The measured results of efficiency and receiving power varying with δ are shown in Figure 5. Figure 6 shows the waveforms of the input voltage, input current, and output voltage when the optimal compensation is applied ($@R_{DC} = 5\Omega$ and $@R_{DC} = 10\Omega$). The waveforms are measured using the oscilloscope (Tektronix TDS2014C), the current probe (Sunraise SRS6025) and the voltage probes (Cybertek P1300).

Setting $R_{DC} = 5\Omega$, different coupling conditions are obtained by changing the positions of the three coils. Based on (15) and (17), the optimal compensation factor δ can be 0.1963 (@A: $k_1 = 0.181$, $k_2 = 0.152$, $k_3 = 0.0672$), 0.1074 (@B: $k_1 = 0.125$, $k_2 = 0.128$, $k_3 = 0.045$) and 0.043 (@C: $k_1 = 0.0889$, $k_2 = 0.0798$, $k_3 = 0.0247$). The corresponding compensation capacitors are 523.6, 442.4 and 397.7 nF. The measured results of efficiency and receiving power varying with δ are shown in Figure 7.

According to the experiment results under different load and crossing coupling conditions, the compensation capacitor of RPC influences the efficiency of the three-coil WPT system markedly. For case A

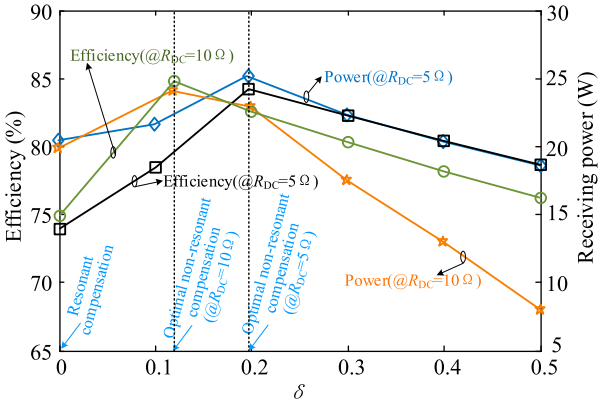

Figure 5. Measured results of efficiency and receiving power varying with δ.

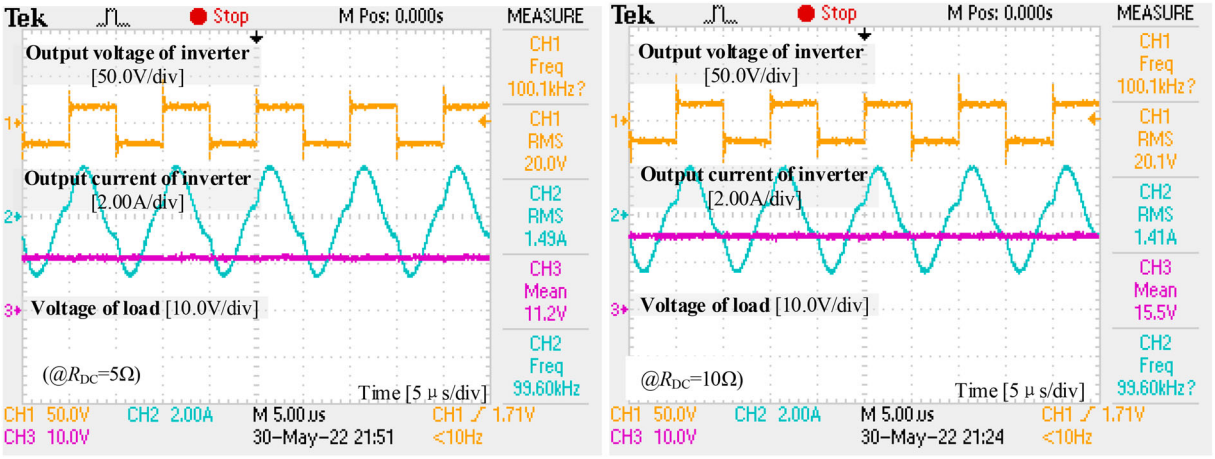

Figure 6. Waveforms when the optimal compensation applied (@R_{DC} = 5Ω and @R_{DC} = 10Ω).

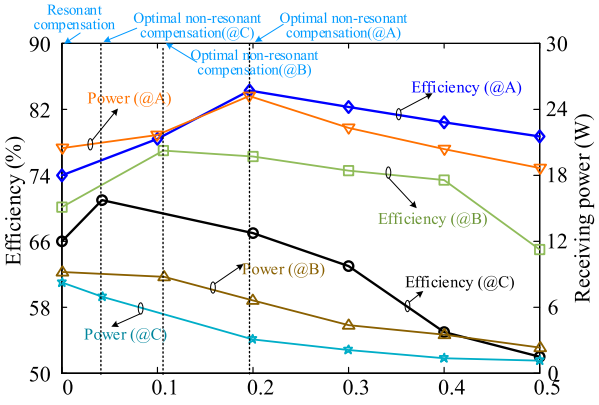

Figure 7. System characteristics under different cross- couplings.

in Figure 7, system efficiency is promoted from 73.9% (resonant compensation) to 84.2% (non-resonant compensation optimization). Higher efficiency is achieved under non-resonant compensation optimized by the theoretical analysis compared to resonant compensation. The theoretical analysis and optimization are verified experimentally under different load or cross-coupling conditions.

5. Conclusions

In a three-coil WPT system, the cross-coupling among three coils, the compensation capacitor of the repeating coil (RPC) and the rectified load are not fully considered simultaneously. In this paper, the circuit model of a three-coil WPT system with a rectified load is developed to analyse the general status by taking the cross-coupling of all coils and the compensation capacitor of RPC into consideration. The internal connection among system efficiency, compensation level and rectifier load is derived. According to the proposed modelling and analysis, it is proved that the optimal efficiency is achieved at resonant compensation theoretically when the coupling between TC and RC is ignored. After taking the coupling between TC and RC into consideration, the detailed mathematical analysis and compensation capacitor selection of RPC are investigated to improve the system efficiency. Finally, the experimental study demonstrates that the selected compensation capacitor of RPC achieves a higher efficiency than the resonant compensation in a three-coil WPT system with different cross-coupling conditions and rectifier load conditions.

Disclosure statement

No potential conflict of interest was reported by the author(s).

Funding

This work was supported in part by the National Natural Science Foundation of China (52107003), in part by the Chinese Postdoctoral Science Foundation (2021M690867), in part by the Postdoctoral Fund of Jiangsu Province (2021K030A), in part by the Project of Jiangsu Provincial Key Laboratory of Smart Grid Technology and Equipment in Southeast University, in part by the Fundamental Research Funds for the Central Universities (B200201018), and in part by the Project of science and technology innovation for overseas returnees in Nanjing (B2004805).

References

[1] Tan L, Li C, Li J, et al. Mesh-based accurate positioning strategy of EV wireless charging coil with detection coils. IEEE Trans Ind Inf. 2021;17(5):3176–3185. DOI:10.1109/TII.2020.3007870

[2] Hasanzadeh S, Vaez-Zadeh S. A review of contactless electrical power transfer: applications, challenges and future trends. Automatika. 2015;56(3):367–378. DOI:10.7305/automatika.2015.12.727

[3] Wang R, Tan L, Li C, et al. Analysis, design, and implementation of junction temperature fluctuation tracking suppression strategy for SiC MOSFETs in wireless high-power transfer. IEEE Trans Power Electron. 2021;36(1):1193–1204. DOI:10.1109/TPEL.2020.3004922

[4] Zhang X, Wang F, Ni X, et al. Structure electromagnetic force analysis of WPT system under

fault conditions. IEEE Access. 2020;8:152990–153000. DOI:10.1109/ACCESS.2020.3015278

[5] Puttananjegowda K, Cao Y, Greenv M. DC-DC boost converter for wireless power transfer systems. 2021 IEEE 12th Annual Ubiquitous Computing, Electronics & Mobile Communication Conference (UEMCON), New York, NY, USA; 2021. p. 0661–0665. DOI:10.1109/UEMCON53757.2021.9666551

[6] Zhang P, Yang Q, Zhang X, et al. Comparative study of metal obstacle variations in disturbing wireless power transmission system. IEEE Trans Magn. 2017;53(6):1–4. Art no. 9100304. DOI:10.1109/TMAG.2017.2657517

[7] Song K, Yang G, Zhang H, et al. An impedance decoupling-based tuning scheme for wireless power transfer system under dual-side capacitance drift. IEEE Trans Power Electron. 2021;36(7):7526–7536. DOI:10.1109/TPEL.2020.3043229

[8] Yang G, Song K, Huang X, et al. Improved interoperability evaluation method for wireless charging systems based on interface impedance. IEEE Trans Power Electron. 2021;36(8):8588–8592. DOI:10.1109/TPEL.2021.3053353

[9] Chittoor PK, Bharatiraja C. Solar integrated wireless drone charging system for smart city applications. 2021 IEEE 6th International Conference on Computing, Communication and Automation (ICCCA), Arad, Romania; 2021. p. 407–412. DOI:10.1109/ICCCA52192.2021.9666263

[10] Liu H, Huang X, Tan L, et al. Dynamic wireless charging for inspection robots based on decentralized energy pickup structure. IEEE Trans Ind Inf. 2018;14(4):1786–1797. DOI:10.1109/TII.2017.2781370

[11] Corti F, Reatti A, Musumeci S. Effects of control strategies on AC-DC conversion efficiency in EV wireless charging. 2021 AEIT International Conference on Electrical and Electronic Technologies for Automotive (AEIT AUTOMOTIVE), Torino, Italy; 2021. p. 1–6. DOI:10.23919/AEITAUTOMOTIVE52815.2021.9662884

[12] Wang W, Xu C, Zhang C, et al. Optimization of transmitting coils based on uniform magnetic field for unmanned aerial vehicle wireless charging system. IEEE Trans Magn. 2021;57(6):1–5. Art no. 8600105. DOI:10.1109/TMAG.2021.3063796

[13] Wang W, Zhang C, Wang J, et al. Multipurpose flexible positioning device based on electromagnetic balance for EVs wireless charging. IEEE Trans Ind Electron. 2021;68(10):10229–10239. DOI:10.1109/TIE.2020.3022490

[14] Wen F, Chu X, Li Q, et al. Optimization on three-coil long-range and dimension-asymmetric wireless power transfer system. IEEE Trans Electromagn Compat. 2020;62(5):1859–1868. DOI:10.1109/TEMC.2020.2976652

[15] Xiao Y, Guan Y, Wang Y, et al. Design and optimization of self-compensating multi-relay wireless power transmission system with metal flanges. 2021 24th International Conference on Electrical Machines and Systems (ICEMS), Gyeongju, Republic of Korea; 2021. p. 716–721. DOI:10.23919/ICEMS52562.2021.9634346

[16] Kiran KBS, Kumari M, Behera RK, et al. Analysis and experimental verification of three-coil inductive resonant coupled wireless power transfer system. 2017 National Power Electronics Conference (NPEC), Pune, India; 2017. p. 84–89. DOI:10.1109/NPEC.2017.8310439

[17] Wang W, Huang X, Pan S, et al. Moving impedance matching analysis for three-coil wireless power transfer system in mid-range. 2016 IEEE 5th Asia-Pacific Conference on Antennas and Propagation (APCAP), Kaohsiung, Taiwan; 2016. p. 429–430. DOI:10.1109/APCAP.2016.7843275

[18] Li Y, Hu J, Liu M, et al. Reconfigurable intermediate resonant circuit based WPT system with load-independent constant output current and voltage for charging battery. IEEE Trans Power Electron. 2019;34(3):1988–1992. DOI:10.1109/TPEL.2018.2858566

[19] Li Y, Xu Q, Lin T, et al. Analysis and design of load-independent output current or output voltage of a three-coil wireless power transfer system. IEEE Trans Transp Electrification. 2018;4(2):364–375. DOI:10.1109/TTE.2018.2808698

[20] Wang W, Huang X, Guo J, et al. Power stabilization based on efficiency optimization for WPT systems with single relay by frequency configuration and distribution design of receivers. IEEE Trans Power Electron. 2017;32(9):7011–7024. DOI:10.1109/TPEL.2016.2626498

[21] Steigerwald RL. A comparison of half-bridge resonant converter topologies. IEEE Trans Power Electron. 1988;3(2):174–182. DOI:10.1109/63.4347

[22] Li S, Li W, Deng J, et al. A double-sided LCC compensation network and its tuning method for wireless power transfer. IEEE Trans Veh Technol. 2015;64(6):2261–2273. DOI:10.1109/TVT.2014.2347006